Copyright © 2008 by the Genetics Society of America
DOI: 10.1534/genetics.108.090951

The Dominant Cold-Sensitive *Out-Cold* Mutants of *Drosophila melanogaster* Have Novel Missense Mutations in the Voltage-Gated Sodium Channel Gene *paralytic*

Helen A. Lindsay,*,†,[1] Richard Baines,‡ Richard ffrench-Constant,§ Kathryn Lilley, Howard T. Jacobs*,† and Kevin M. C. O'Dell*,[2]**

**IBLS Division of Molecular Genetics, University of Glasgow, Glasgow G11 6NU, United Kingdom, †Institute of Medical Technology and Tampere University Hospital, FI-33014 University of Tampere, FI-33014 Tampere, Finland, ‡Faculty of Life Sciences, University of Manchester, Manchester M13 9PT, United Kingdom, §Centre for Ecology and Conservation, Cornwall Campus, University of Exeter, Penryn, Cornwall TR10 9EZ, United Kingdom and **Cambridge Centre for Proteomics, Cambridge System Biology Centre, Department of Biochemistry, University of Cambridge, Cambridge CB2 1QR, United Kingdom*

Manuscript received May 2, 2008
Accepted for publication June 23, 2008

ABSTRACT

Here we report the molecular characterization of *Out-cold* (*Ocd*) mutants of *Drosophila melanogaster*, which produce a dominant, X-linked, cold-sensitive paralytic phenotype. From its initial 1.5-Mb cytological location within 13F1-16A2, *P*-element and SNP mapping reduced the *Ocd* critical region to <100 kb and to six candidate genes: *hangover*, CG9947, CG4420, *eIF2a*, *Rbp2*, and *paralytic* (*para*). Complementation testing with *para* null mutations strongly suggests *Ocd* and *para* are allelic, as does gene rescue of *Ocd* semilethality with a wild-type *para* transgene. Pesticide resistance and electrophysiological phenotypes of *Ocd* mutants support this conclusion. The *para* gene encodes a voltage-gated sodium channel. Sequencing the *Ocd* lines revealed mutations within highly conserved regions of the *para* coding sequence, in the transmembrane segment S6 of domain III (I1545M and T1551I), and in the linker between domains III and IV (G1571R), the location of the channel inactivation gate. The G1571R mutation is of particular interest as mutations of the orthologous residue (G1306) in the human skeletal muscle sodium channel gene *SCN4A* are associated with cases of periodic paralysis and myotonia, including the human cold-sensitive disorder *paramyotonia congenita*. The mechanisms by which sodium channel mutations cause cold sensitivity are not well understood. Therefore, in the absence of suitable vertebrate models, *Ocd* provides a system in which genetic, molecular, physiological, and behavioral tools can be exploited to determine mechanisms underlying sodium channel periodic paralyses.

THE molecular mechanisms underlying cold sensitivity in metazoans are not well understood, not least because relatively few studies have addressed this question. A few cold-sensitive mutations have been described in *Drosophila melanogaster* (Siddiqi and Benzer 1976; Sondergaard 1980; Lilly *et al.* 1994), but again the precise mechanisms by which these specific mutations lead to cold sensitivity have not been elucidated. The objective of this study was to identify the biological processes underlying cold sensitivity.

The dominant cold-sensitive paralytic *Out-cold* (*Ocd*) mutations of *D. melanogaster* were originally isolated in a screen for X-linked male-lethal mutations (Sondergaard 1975, 1979). Further analyses of the male-lethal stocks identified seven lines in which heterozygous mutant females exhibited a dominant cold-sensitive paralysis. Within several of these lines a few mutant males did eclose, but they were weak, uncoordinated, and usually died in the wet food medium before they had the opportunity to mate. However, rare surviving males allowed crosses between strains to be undertaken and the seven apparently independently derived mutations were shown to be allelic. The seven mutant alleles of *Ocd* were designated Ocd^{1} to Ocd^{7} (Sondergaard 1975, 1979).

The effect of temperature on the *Ocd* mutant phenotype has been investigated in considerable detail (Sondergaard 1975). At 4°, all *Ocd* males are paralyzed within 1 min. Upon exposure to cold shock, *Ocd* mutants display paralysis-associated phenotypes such as leg shaking and wing flutter. Heterozygous (*Ocd*/+) females and the more severely affected rare hemizygous (*Ocd*/Y) males display reversible cold-sensitive paralysis. The survival of hemizygous mutant males is temperature dependent, with Ocd^{2} males eclosing from stocks maintained at 25°, but not at 18°. Surviving *Ocd* males walk in a reeling manner and are usually unable to fly, although the mutant phenotype varies greatly between

[1]*Present address:* Yorkshire Regional DNA Laboratory, St James's University Hospital, Leeds, UK, LS9 7TF.

[2]*Corresponding author:* IBLS Division of Molecular Genetics, Anderson College Complex, University of Glasgow, 56 Dumbarton Rd., Glasgow G11 6NU, UK. E-mail: k.odell@bio.gla.ac.uk

individual flies. With respect to cold sensitivity and male viability, there is considerable variation between the mutant alleles in the severity of the phenotype (Sondergaard 1975, 1979). However, whether the phenotypic variation in severity is a property of the allele itself, or associated with the acquisition of modifier mutations in laboratory stocks, is at this stage unclear.

Initial investigations into the molecular basis of the *Ocd* cold-sensitive paralysis involved the study of the reaction kinetics of the mitochondrial enzyme complex succinate cytochrome c reductase (SCCR), which reflects the combined enzyme activity of complexes II and III of the respiratory chain (Sondergaard *et al.* 1975). Upon temperature decrease from 25° to 18–20°, abrupt changes in SCCR activation energy were observed in all *Ocd* lines tested (Sondergaard 1975, 1976, 1979), which correlates with the restrictive temperature for paralysis. This change in activation energy was also observed in wild-type flies, but occurs at a much lower temperature, 8°, below which wild-type flies also eventually succumb to paralysis. Furthermore, 2D gel electrophoresis apparently identified an abnormal pattern of mitochondrial polypeptides in *Ocd* adults (Sondergaard 1986), further implicating the *Ocd* gene product in mitochondrial function. However, it is equally possible that the mitochondrial defect is a downstream effect of susceptibility to cold-induced paralysis, rather than a direct result of the *Ocd* mutations themselves.

Classical genetic mapping using deletions and duplications placed the *Ocd* mutations within 13F1-16A2, a broad region on the X chromosome encompassing several hundred genes (Sondergaard 1975). Two recessive temperature-sensitive paralytic mutants, *paralytic*^{ts1} (*para*^{ts1}) and *shibire*^{ts} (*shi*^{ts}), and the leg-shaking mutant *Hyperkinetic* (*Hk*), were crossed to *Ocd*^{1}, but no evidence of allelism was revealed (Sondergaard 1975).

Although there may be only one X-linked gene that mutates to result in dominant cold-sensitive paralysis (Sondergaard 1979), mutations in other X-linked genes do lead to recessive cold sensitivity. For example *comatose* (*comt*), which encodes an N-ethylmaleimide-sensitive fusion protein and is important for neurotransmitter secretion (Ordway *et al.* 1994; Dellinger *et al.* 2000), shows recessive cold-sensitive paralysis (Siddiqi and Benzer 1976). However, *comatose* maps genetically to 11E8, too far a distance from *Ocd* for the two to be allelic. A second X-linked mutant, *hypoactive D* (*hypoD*), which exhibits recessive cold-sensitive paralysis at 15° and maps within the *Ocd* region at 13F1-14B2, is an allele of *slow receptor potential* (*slrp*) (Homyk and Pye 1989). However, *slrp* has not yet been cloned.

Several temperature-sensitive paralytic Drosophila mutants have been isolated with malfunctions in ion pumps or channels. This includes recessive mutations in the voltage-gated calcium channel gene *cacophony* (*cac*) (Kawasaki *et al.* 2000) and the voltage-gated sodium channel gene *paralytic* (*para*) (Loughney *et al.* 1989). A *P*-element insertion in the sodium pump α-subunit gene has also been shown to result in recessive cold-sensitive lethality (Feng *et al.* 1997). The *para* gene encodes the major functional voltage-gated sodium channel in Drosophila (Loughney *et al.* 1989) and two *para* mutants isolated in screens for smell insensitivity, *para*^{smellblind1} and *para*^{smellblind2}, are associated with recessive cold-sensitive lethality (Lilly *et al.* 1994). The *para* gene lies within the *Ocd* critical region, and several previously characterized *para* mutations exhibit heat-sensitive paralysis (Suzuki *et al.* 1971; Loughney *et al.* 1989). However, while *para* is an attractive candidate host of the *Ocd* mutation, it was previously excluded on the basis of complementation tests (Sondergaard 1975). Nevertheless a cold-sensitive human disorder associated with mutations of a sodium channel gene manifests as the rare autosomal dominant muscle disease *paramyotonia congenita* (Ptacek *et al.* 1992).

D. melanogaster models of genetic disease have proven to be invaluable in elucidating the pathogenic mechanisms behind many human disorders (Fortini and Bonini 2000; Kornberg and Krasnow 2000; Zoghbi and Botas 2002; O'Kane 2003; Jacobs *et al.* 2004; Bier 2005; Chintapalli *et al.* 2007). Such models therefore have the potential to aid the development of therapeutic interventions. Here we report the molecular and phenotypic characterization of the Drosophila *Out-cold* (*Ocd*) mutations, and speculate on how they may be exploited as a tool with which to investigate human disorders associated with seizures, paralysis, and cold sensitivity.

MATERIALS AND METHODS

Drosophila stocks: Fly stocks were maintained in plastic vials or bottles (for large-scale amplification) containing food medium (1% (w/v) bacto-agar, 1.5% (w/v) sucrose, 3% (w/v) glucose, 3.5% (w/v) active dried yeast, 1.5% (w/v) maize meal, 1% (w/v) wheat germ, 1% (w/v) soya flour, 3% (w/v) treacle, 0.5% (v/v) propionic acid, 0.1% (w/v) nipagin M in H_2O). Stocks were reared at 25° unless otherwise stated, with ambient humidity on a 12/12 hr light/dark cycle. Basic techniques for the laboratory culture of Drosophila were as described by Ashburner (1989). In fly crosses, six females were crossed with six males of the required genotype in each vial. The parent flies were removed prior to the next generation hatching.

The wild-type control strains, Oregon-R and Canton-S, have been maintained as mass-bred stocks in the O'Dell laboratory in Glasgow for many years. The generation of the EMS-induced *Ocd* lines has been described previously (Sondergaard 1975, 1979). The recessive lethal strain *para*$^{Df(1)D34}$ contains an internal deletion within *para* that causes a null mutation (Broadie and Bate 1993). The *hangover*^{AE10NT} strain has a *P*-element insertion within the coding region of the first exon of *hangover* (*hang*), causing an abnormal response to environmental stressors such as ethanol and paraquat (Scholz *et al.* 2005) and was kindly provided by H. Scholz. The *slrp*^{4} strain has an EMS-induced mutation in the *slow receptor potential* gene (Homyk and Pye 1989).

For the gene rescue experiments, the *para* strain *P*{UAS-*para13.5*} was used to expresses *para* splice variant 13.5 under

P{GAL4} control (Warmke *et al.* 1997). UAS-*para13.5* was produced via standard methods from a *para13.5*-containing *p*GH19 construct kindly provided by J. Warmke. The *P*{GAL4} lines used to drive *P*{UAS-*para13.5*} were *P*{GAL4-*Heat-shock protein 70.PB*} (Jarman *et al.* 1993), *P*{GAL4-*daughterless.G32*} (Wodarz *et al.* 1995), *P*{GAL4-*1407*} (Sweeney *et al.* 1995), *P*{GAL4-*Myocyte enhancing factor 2.R*} (Ranganayakulu *et al.* 1996), and *P*{GAL4-*eyeless*} (Bonini *et al.* 1997). The *P*-element insertion lines used for red/white selection in mapping *Ocd*, *P*{*SUPor-P*}*kat80*^{KG02315}, *P*{*EPgy2*}*EY04615*, *P*{*EPgy2*}*EY3459*, *P*{*EPgy2*}*CG4239*^{EY01983}, and *P*{*GT1*}*BG00710*, were obtained from the Berkeley Drosophila Genome Project (BDGP) Gene Disruption Project (Bellen *et al.* 2004).

The *Out-cold* strains have been kept in isolation since their creation (L. Sondergaard, personal communication). While they retain their cold sensitivity, it is very likely, even in a balanced stock where the mutant *Ocd* allele is usually present only in a heterozygous state, that selection will act to modify and mollify the dominant mutant phenotype. To address this the strains were isogenized into two wild-type backgrounds, Canton-S and Oregon-R. To avoid problems with selection, the *Ocd* mutations were isogenized using chromosome replacement. Note that the isogenized strains retain their original *Ocd* mutant X chromosome. Therefore ~80% of the isogenized strain is from the wild-type Canton-S or Oregon-R line (chromosomes 2 and 3), and 20% (the X chromosome) is from the original *Ocd* strain.

SNP mapping: Sequencing coding and noncoding regions of genes in the original *Ocd* critical region (13F1-16A2) identified eight SNPs distinguishing the *Ocd*^{1} and Oregon-R (ORR) strains (Table 1). The SNPs were identified during sequencing coding and noncoding regions of "mitochondrial" candidate genes within the original *Ocd* critical region (13F1-16A2). This identified SNPs in CG9240, CG8288 (*mRpL3*), CG8931, CG3525 (*eas*), and CG3560. To fill in appropriate gaps for fine recombination SNP mapping, SNPs were subsequently identified in *disco-r*, *para*, and *rudimentary*. Flies carrying a recombinant *Ocd*/ORR chromosome were generated, and in these the eight SNPs were genotyped using the ABI Prism SNaPshot primer extension kit (Applied Biosystems). The genotypes and phenotypes of recombinant flies allow an estimation of the relative position of *Ocd*^{1} to specific SNPs.

***P*-element mapping:** Using red/white selection (Zhai *et al.* 2003), the *Ocd* mutation was mapped relative to five molecularly defined *P*-element insertions obtained from the BDGP Gene Disruption Project (Bellen *et al.* 2004). Insertion sites were confirmed using inverse PCR, according to the BDGP protocol. The *Ocd*^{1} mutation was crossed into a *w*^{1118} background. Flies recombinant between *Ocd*^{1} and each *P*-element insertion were generated. The presence of each *P*-element was scored by the expression of the *white* gene. Presence of the *Ocd*^{1} mutation was scored by tests for cold sensitivity (at 4°). Genetic distances between *Ocd* and each *P*-element were calculated from the proportions of recombinant flies observed. Standard errors were calculated as the square root of PQ/n, where P is the percentage of recombinant genotypes, Q is the percentage of parental genotypes, and n is the sample size.

Gene rescue: Flies carrying the construct *P*{UAS:*para*$^{+}$} on either the second or third chromosome were crossed to *Ocd*^{1} flies using appropriate balancer chromosomes to generate *Ocd*^{1}/FM7; *P*{UAS:*para*$^{+}$}; + or *Ocd*^{1}/FM7; + ; *P*{UAS:*para*$^{+}$} females. In gene rescue crosses, these females were crossed to male flies that either were wild type (Canton-S or Oregon-R) or carried a *P*{GAL4} construct that directs wild-type *para* expression in a specific spatial and temporal pattern. The number of *Ocd*^{1} and FM7 males eclosing over 4 days from the first eclosion were counted, and the percentage of males carrying the *Ocd*^{1} mutant allele was calculated. Standard error of the proportion for each value was calculated as the square root of PQ/n, where P is the percentage of *Ocd*^{1} eclosing, Q is the percentage of FM7 males eclosing, and n is the sample size. 2×2 χ^2-analysis was performed on the raw data to test for significant deviation from the pooled wild-type (Canton-S and Oregon-R) results.

DNA sequencing: DNA sequencing reactions on purified PCR products were carried out by the Molecular Biology Support Unit at the University of Glasgow on a MegaBACE 1000 capillary sequencer (Amersham) using Big Dye chemistry (Applied Biosystems). Sequences were analyzed using ABI Prism EditView or 4peaks software.

Electrophysiology: Electrophysiology experiments were performed using protocols described previously (Baines and Bate 1998; Mee *et al.* 2004). Voltage steps of 15 mV increments were applied to cells from a conditioning potential of −90 mV (steps ranged from −60 to +45 mV). To better resolve Na^{+} currents, an on-line leak subtraction protocol was used (P/4). Currents measured are the averages of five trials for each cell. Recordings were taken from aCC and RP2 neurons in first instar at three temperatures: 16°, 22°, and 28°. However, all larvae were raised at 25°. Student's *t*-tests were used to test for significant deviation from wild type.

DDT bioassay: For DDT bioassays, 20 adult flies <72 hr posteclosion were placed in glass vials with interior surfaces evenly coated with varying concentrations of DDT (Sigma) dissolved in 200 μl acetone and allowed to air dry. The vials were sealed with cotton wool soaked in 5% sucrose solution. Mortality was scored after 24 hr with flies being unable to move being scored as dead. Dose-response curves were estimated from six different concentrations of DDT with three replicates per dose. Probit analysis was performed using the computer program POLO (Robertson *et al.* 1980).

Proteomics: Protein was extracted from 12 adult male Drosophila aged between 1 and 2 days using protocols and statistical analyses described previously (Karp *et al.* 2005). Protein concentration was determined at the Cambridge Centre for Proteomics (CCP) using the BioRad DC protein assay (Bio-Rad). 2D DIGE was performed at the CCP as described previously (Swatton *et al.* 2004). The DeCyder version 4 Biological Variation Analysis (BVA) (GE Healthcare) software module was used to identify spots with increased or decreased expression between samples, on the basis of calculated standardized abundances. Standardized abundance was calculated by dividing spot volumes by the Cy2 internal standard for each spot. Statistical analysis was applied using standard ANOVA (Karp *et al.* 2005). Spots with $P < 0.05$ for random occurrence were considered to differ significantly between samples. Protein gels were fixed and stained using Colloidal Coomassie Brilliant Blue and spots of interest excised manually within a laminar flow cabinet. Mass spectrometry to identify proteins from 2D DIGE experiments was performed at the CCP. Protein spots within the gel were first reduced, carboxyamidomethylated, and then digested to peptides using trypsin on a MassPrepStation (Waters, Manchester, UK), before being applied to LC-MS/MS. For LC-MS/MS, the reverse phase liquid chromatographic separation of peptides was achieved with a PepMap C18 reverse phase, 75 μm i.d., 15-cm column (LC Packings, Amsterdam) on a capillary LC system (Waters) attached to QTof2 (Waters) mass spectrometer. The MS/MS fragmentation data achieved was used to search the National Center for Biotechnology Information (NCBI) database using the MASCOT search engine (http://www.matrixscience.com).Probability-based MASCOT scores were used to evaluate identifications. Only matches with $P < 0.05$ for random occurrence were considered

TABLE 1

SNPs identified across the Ocd region

Gene	Map location and gene orientation (forward or reverse strand)	SNP location	Position of SNP in gene	Flanking sequence	*Ocd*^{1}	ORR
CG9240	13E8 Reverse	AE003499.5 nt 5748	110 bp 3′ of gene	AAATG-TATCA	C	G
mitochondrial ribosomal protein L3 (*mRpL3*)	13E14 Forward	AE003500.4 nt 55600	Intron 1	ATGCG-AGCGT	T	G
CG8931	14A5 Forward	AE003500.4 nt 277193	838 bp 5′ of gene	AGCAG-CGAAC	A	C
disco-related (*disco-r*)	14B1 Reverse	AE003501.4 nt 213518	Exon 2	CCGGA-TGCCG	T	C
easily shocked (*eas*)	14B7 Forward	AE003501.4 nt 272377	Intron 2	ACGAA-CCATC	A	T
CG3560	14B8 Forward	AE003501.4 nt 277695	Exon 3	AAGGA-GCCGT	A	G
paralytic (*para*)	14D1-14E1 Reverse	AE003502.4 nt 123890	Intron 6	GTAAC-CCCAA	G	C
rudimentary (*r*)	14F5-15A1 Forward	AE003503.4 nt 28093	Intron 5	AACGA-TTAAT	C	T

Eight identified SNPs are shown, together with their cytogenetic map position (FlyBase: http://flybase.bio.indiana.edu), orientation on the X chromosome (forward or reverse strand), and the nucleotide (nt) position of each SNP in the corresponding NCBI GenBank *Drosophila melanogaster* genomic scaffold (AE no.), and the position of the SNP relative to the associated gene. Where the gene is transcribed on the reverse strand, the nucleotide position refers to that of the reverse complemented strand. The flanking sequence of each SNP is also shown, along with the base present in either *Ocd*^{1} or wild-type Oregon-R DNA.

significant (further explanation of MASCOT scores can be found at http://www.matrixscience.com).

RESULTS

***Out cold* is allelic to the voltage-gated sodium channel gene *paralytic*:** Genes that mapped within the *Ocd* critical region (13F1-16A2) and were considered to be directly or perhaps indirectly involved in mitochondrial function were sequenced. In the *Ocd*^{1} strain none of the five candidate genes, *CG9240*, *mitochondrial ribosomal protein L3*, *CG8931*, *easily shocked*, and *CG3560*, had coding mutations (Table 1). However, noncoding SNPs from each of the five genes were identified and, coupled with SNPs from three other genes, *disco-r*, *paralytic* (*para*), and *rudimentary*, were used to facilitate more precise mapping of *Ocd*. In addition, crosses performed between mutant alleles of *Ocd* and *slrp* (*hypoD*) did not provide any evidence that the two mutations are allelic (data not shown).

The *Ocd* (13F1-16A2) region of the X chromosome represents ~2% of the fly genome, and ~300 genes. Five *P*-element insertions (Figure 1) and eight SNPs (Table 1) were used to identify the position of the *Ocd* mutation more precisely. This identifies an insertion 5′ of the 5′-UTR of *hangover* (*hang*) and a SNP within intron 6 of *para* as the closest upstream and downstream flanking markers of *Ocd* (Figure 2). This mapping confined the *Ocd* critical region to only six candidate genes, *hang*, CG9947, CG4420, *eIF2a*, *Rbp2*, and *para*. Sequencing the coding regions of the first five of these genes in *Ocd*^{1} failed to find any mutations affecting their amino acid sequences.

Complementation tests are complicated by the fact that *Ocd* cold sensitivity is dominant. In addition, of the six candidate genes, mutant strains are only available for *hangover* and *para*. However, hemizygous *Ocd*/Y males and homozygous *Ocd*/*Ocd* females exhibit recessive semilethality and a recessive droopy wing phenotype.

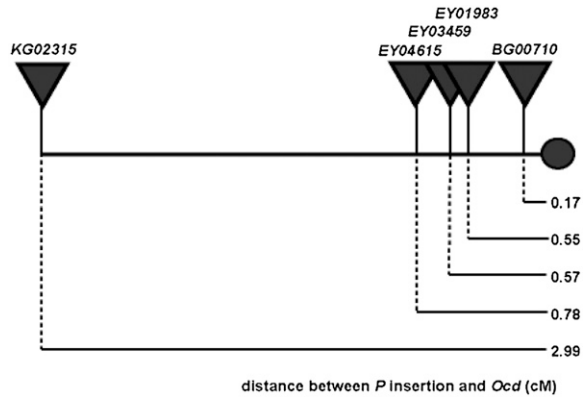

FIGURE 1.—The *Ocd* region showing relative positions of *P*-element insertions. *P* elements are represented by inverted triangles; the *Ocd* gene is represented by a circle. The map shows relative positions and the calculated genetic distances (cM) between each *P*-element insertion and *Ocd*.

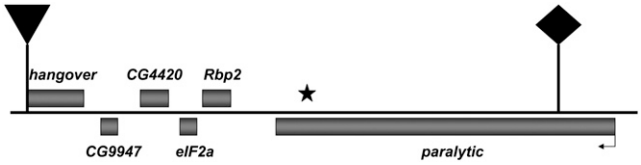

FIGURE 2.—Topographical representation of the *Ocd* region. The *Ocd* region encompasses six genes over the 100-kb 14C6–14E1 region. The *para* gene is ~64 kb of the region. The *P* element defining the left-hand limit (BDGP line BG00710) is represented by an inverted triangle. The SNP defining the right-hand limit (AE003502.4 nt 123890 G/C; intron 6 of *para*) is indicated by a diamond. The arrow indicates the direction of transcription of *para*. The approximate position of the three *Ocd* point mutations is shown by a star.

Therefore we would expect females heterozygous for a cold-sensitive *Ocd* allele and an *Ocd* null allele to have a similar semilethal and droopy wing phenotype. Irrespective of the temperature they are grown at, *Ocd/hang* females derived from *Ocd*/FM7 mothers and *hang*/Y fathers are cold sensitive (due to the *Ocd* dominant cold sensitivity). In addition they are viable and fertile and exhibit no other obvious mutant phenotypes, providing no evidence that *Ocd* and *hang* are allelic. However, the phenotype of *Ocd*/*para*$^{Df(1)D34}$ females depended on the temperature at which they were generated. When conceived and raised at 25° *Ocd*/*para*$^{Df(1)D34}$ females were cold sensitive and indistinguishable from their *Ocd*/+ sisters. However, when conceived and raised at 18° *Ocd*/*para*$^{Df(1)D34}$ females displayed phenotypes distinct from that of either heterozygous parent in that they were uncoordinated, holding their wings down in a drooped position, and were generally unfit, manifesting a phenotype that is remarkably similar to that of *Ocd*/Y mutant males (Figure 3, A and B). Given that *para*$^{Df(1)D34}$ is a null internal deletion of *para*, this strongly suggests *Ocd* and *para* are allelic.

Gene rescue: Proof that the *Ocd* mutations are in the *para* gene can only be demonstrated by gene rescue, where expression of a wild-type *para* transgene in an *Ocd* mutant reverts the host fly to a wild-type phenotype. Again this is complicated by the fact that the primary *Ocd* phenotype, cold sensitivity, is dominant. However, *Ocd*^{1}/FM7 mothers produce sons in the ratio of ~9 FM7/Y to 1 *Ocd*^{1}/Y rather than the expected 1:1, a phenotype described as semilethality. It is therefore theoretically possible to assay for any *para*-mediated rescue of *Ocd*^{1} male semilethality, by expressing the wild-type *para* transcript, which would be expected to restore the ratio of FM7/Y to *Ocd*^{1}/Y males to ~1:1. Gene rescue is further complicated by the size, splicing complexity, and RNA-editing of the *para* transcript. Given these complicating factors, we felt there was little prospect of achieving complete gene rescue, but nevertheless introduced *para13.5* transgenes into *Ocd*^{1} stocks in the hope of detecting a significant shift from a 9:1 toward a 1:1 ratio.

For all four *P*{GAL4} drivers used to drive *UAS-para13.5*, χ^2 tests reveal a significant increase ($P < 0.001$) in the number of *Ocd*^{1}/Y males eclosing (Figure 4). The fact that *para* expression significantly rescues the viability of *Ocd*^{1}/Y males strongly suggests that *Ocd* and *para* are allelic. Perhaps surprisingly, the observed rescue in the viability of *Ocd*^{1}/Y males does not seem to discriminate between the different categories of *P*{GAL4} driver used. As para is normally expressed neuronally it is expected that *P*{*1407*:GAL4}-driven expression of *para*$^{+}$ panneurally would result in rescue, as would ubiquitous *P*{*da*:GAL4}-driven expression of *para*$^{+}$. However, it is difficult to explain why expression of *para*$^{+}$ in the muscle by *P*{*dmef2*:GAL4} or in the eye discs by *P*{*ey*:GAL4} also results in significant rescue. One possible explanation is that the *P*{GAL4} drivers may not be as restricted in their expression pattern as previously described. Interestingly, relative to wild-type controls neuronal excitability, itself dependent on *para* expression, is increased in *UAS-para13.5* stocks even in the absence of a *P*{GAL4} driver (R. BAINES, unpublished data).

***Ocd* strains show missense mutations in highly conserved regions of *para*:** Sequencing of coding regions of the *para* gene revealed missense mutations within exon 28 in six of the *Ocd* strains, but no coding mutations were found elsewhere. The mutations uncovered were I1545M and G1571R, somewhat surprisingly occurring as a double mutation in *Ocd*^{1}, *Ocd*^{3}, *Ocd*^{5}, *Ocd*^{6}, and *Ocd*^{7}, and T1551I in *Ocd*^{2} (Figure 5). None of

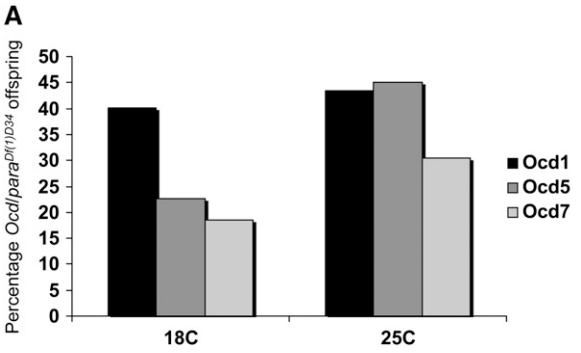

FIGURE 3.—Noncomplementation of *Ocd* and *para*$^{Df(1)D34}$. (A) If there was complementation between *Ocd* and *para* we would expect similar frequencies (50%) of *Ocd*/*para*$^{Df(1)D34}$ and *Ocd*/FM7 daughters. At 25° there is a significant deficit of *Ocd*^{7}/*para*$^{Df(1)D34}$ daughters ($\chi^2 = 12.16$, $P < 0.005$). At 18° there is a significant deficit of all *Ocd*/*para*$^{Df(1)D34}$ daughters (*Ocd*^{1} $\chi^2 = 6.52$, $P < 0.05$; *Ocd*^{5} $\chi^2 = 28.96$, $P < 0.005$; *Ocd*^{7} $\chi^2 = 26.28$, $P < 0.005$). (B) All females with the *Ocd*^{7}/*para*$^{Df(1)D34}$ genotype have the droopy-winged phenotype that is typical of *Ocd*^{7}/Y mutant males.

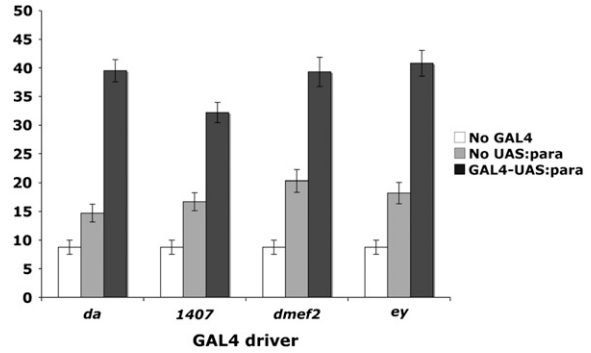

FIGURE 4.—Rescue of Ocd^1/Y semilethality by *P*{GAL4}-mediated expression of para$^+$. Relative percentages of Ocd^1/Y and FM7/Y males in the presence of named *P*{GAL4} drivers, *P*{UAS$_G$:*para*$^+$} or both. χ^2 tests reveal that the relative percentage of Ocd^1/Y males eclosing is significantly higher when the *para* transgene is expressed ($P < 0.001$).

these base-pair changes have been observed in any of the control lines tested, including the original progenitor Oregon-R stock. No mutation was found within the coding region of *para* in Ocd^4. However, on closer investigation the Ocd^4 strain exhibited male lethality without the expected dominant cold sensitivity and was not used further in this study.

Amino acid sequence alignment of Para and the human voltage-gated sodium channels reveals striking similarity. Indeed, Para is 45% identical to the skeletal muscle sodium channel gene SCN4A, and the neural genes SCN1A and SCN2A, and 44% identical to the cardiac sodium channel gene SCN5A. The I1545M and T1551I *Ocd* mutations, caused by A-G and C-T transitions, respectively, both lie at the intracellular phase of segment S6 of domain III of the sodium channel. This is a highly conserved region and each of the three residues mutated in *Ocd* is conserved from Drosophila to man (Figure 5). The G1571R *Ocd* mutation, caused by a G-C transversion, resides within the cytoplasmic linker between domains III and IV, which contains the putative inactivation gate.

***Ocd* larval motor neurons have reduced voltage-gated sodium currents:** Previous analyses of human SCN4A derived from myotonic patients indicate that single amino acid substitutions change the activation threshold and/or rate of fast inactivation. A voltage clamp study was therefore undertaken to study the electrophysiological phenotype of Ocd^1 (I1545M and G1571R) mutant larvae. Whole cell recordings were taken from wild-type and homozygous Ocd^1/Ocd^1 first instar larvae at three temperatures (16°, 22°, and 28°) to assess any temperature sensitivity. Recordings were taken from aCC or RP2 motor neurons, which do not differ in sodium conductance (INa). Peak transient INa was recorded at a range of voltages from −60 to 45 mV (in 15-mV steps). At each temperature, the sodium current-voltage relationships for INa were significantly reduced in Ocd^1 larvae (Figure 6). This reduction is, however, more marked at 16° than at 28°, showing that INa is cold sensitive in these mutants ($P < 0.05$ at 22° and 28°, $P < 0.001$ at 16°). While temperature does not seem to have a great affect on wild-type currents, Ocd^1 larvae display striking cold sensitivity. Analyses of current-voltage relationships, however, show no evidence for any change in activation voltage (Figure 6, C–E). This would

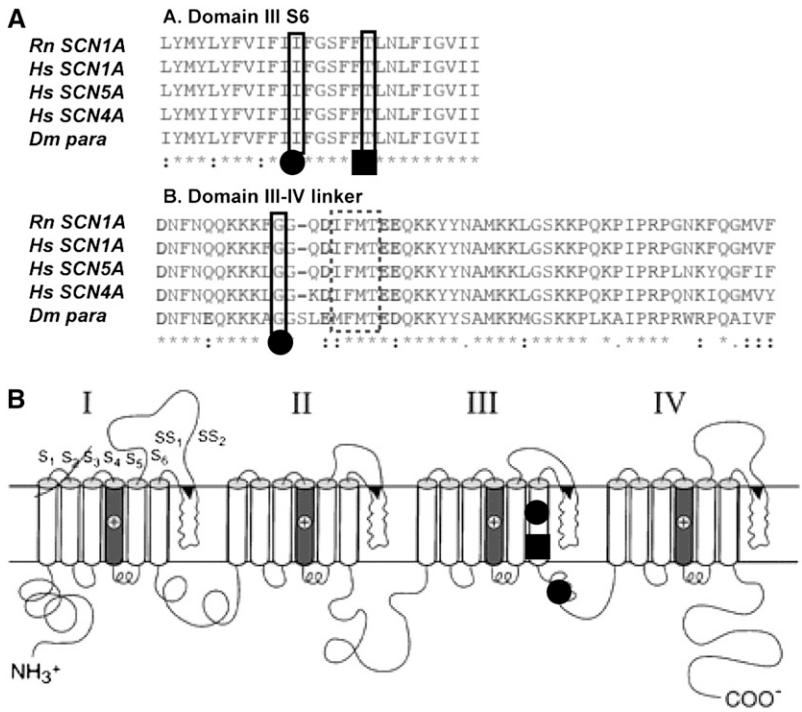

FIGURE 5.—Positions of *Ocd* mutations within Para. (A) Amino acid changes caused by *Ocd* mutations within specific domains of Para. The conserved IFMT box is also highlighted. (B) Positions of *Ocd* mutations on the Para sodium channel Ocd^1 double missense mutation shown as dark circles; Ocd^2 single missense mutation shown as dark square.

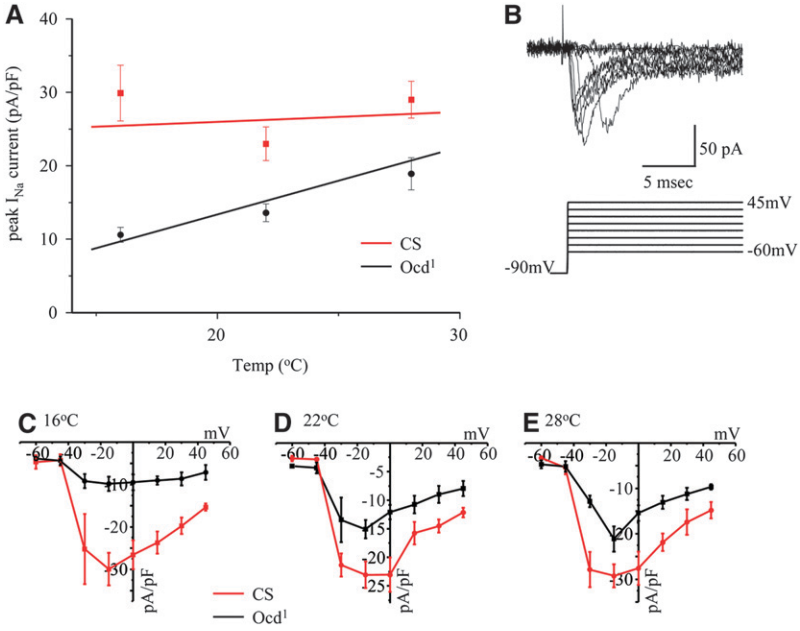

FIGURE 6.—INa is substantially reduced and shows cold sensitivity in *Ocd*^{1} homozygous mutant females. (A) Peak transient INa is significantly reduced in *Ocd*^{1} mutants at the three test temperatures used (16, 22, and 28°). (B) A typical voltage clamp recording of INa from an aCC motoneuron in a wild-type and *Ocd*^{1} mutant first instar larva (22°). (C–E) Current-voltage plots for INa in both wild-type and *Ocd*^{1} mutants at the three test temperatures. For all experiments $n \geq 5 \pm$ SE. CS, Canton-S wild type.

suggest that the reduction in current flow is not due to changes in membrane voltage required for channel opening. The amino acid changes in *Ocd*^{1}, particularly the G to R substitution in the III-IV linker (see Figure 5), are very close to the IFMT sequence that is a component of the fast inactivation particle that allows opened channels to close (*i.e.*, inactivate) within a few milliseconds and to remain closed until membrane potential repolarizes. It is possible, therefore, that either one of these changes might reduce inward INa by increasing the speed of onset of fast inactivation. Further analysis will be needed to clarify whether this is indeed the case or whether current reduction is due to other mechanisms (such as reduced channel density).

***Ocd* mutants show altered resistance to DDT:** Because *Ocd* mutant lines encode sodium channels that differ at single-amino-acid sites, they may respond to specific neurotoxins in a novel fashion. Several neurotoxins, including DDT, target the S6 segment of domain III, the site of two of the three *Ocd* missense mutations identified, I1545M and T1551I. To test for resistance, *Ocd* flies were subjected to a standard DDT contact assay. Relative to the *Ocd* progenitor Oregon-R control, heterozygous *Ocd*^{2}/+ (T1551I/+) females appear to show a mild DDT sensitivity (0.19 resistance compared to wild type), whereas *Ocd*^{5} (I1545M and G1571R) females display a remarkable 1000-fold increase in resistance (Figure 7 and Table 2). The I1545M mutation lies within domain III S6 and the G1571R substitution in the domain III-IV linker. This suggests that the I1545 and/or G1571 residues may be crucial novel targets for DDT.

Several mitochondrial proteins are differentially expressed in *Ocd* flies: To determine, using state-of-the-art methods, whether *Ocd* mutants have a mitochondrial phenotype as reported previously, a comparative proteomics (2D DIGE) study was performed. In 2D DIGE, samples are labeled with spectrally distinct fluorescent dyes and run together on the same gel to overcome problems of reproducibility and intergel variability. The *Ocd*^{2} mutation (T1551I) was selected for analysis as this line yields the most viable males and also because these male flies display mutant phenotypes even at the permissive temperature of 25°. Protein analysis was performed on isogenized whole adult flies controlled for all aspects of environment. All flies were grown at 25° and protein was extracted in three biological replicates per line. Following gel electrophoresis and image analysis using DeCyder software, protein spots showing changes in abundance between wild-type and *Ocd*^{2} males were excised from the gel and identified using mass spectrometry. In total, >40 protein differences were identified. Of these, 22 were successfully

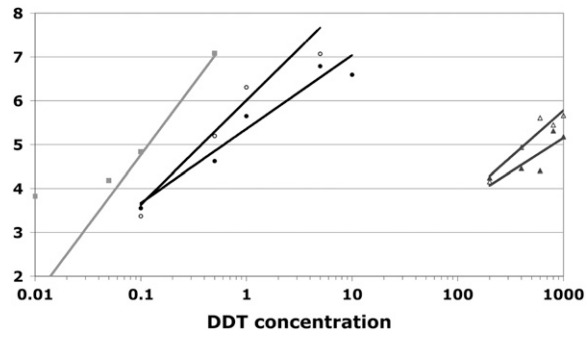

FIGURE 7.—DDT mortality assay in wild-type and *Ocd* mutants. Probit analysis of dose-response relationships for wild-type and *Ocd* mutants. Wild type (circles), *Ocd*^{2} (squares), *Ocd*^{5} (triangles): females (closed), males (open). *Ocd*^{2} males are not viable; *Ocd*^{2} females are heterozygous.

TABLE 2

Resistance levels of wild-type and *Ocd* lines to DDT

Line	Sex	LD_{50} (μg/vial) (95% C.I.)	Resistance ratio
Oregon-R	Male	0.38 (0.21–0.54)	1.00
	Female	0.62 (0.31–1.00)	1.00
Ocd²/FM7	Female	0.12 (0.08–0.16)	0.19
Ocd⁵	Male	432.72 (330–530)	1138.74
	Female	801.67 (550–1720)	1293.02

LD_{50} was calculated for wild-type Oregon-R males and females, heterozygous *Ocd²* females (T1551I), and homozygous *Ocd¹* males and females (I1545M and G1571R). *Ocd²* homozygous females and hemizygous males are lethal, so no data were available. Confidence intervals (95%) are displayed. For each test group, $n = 360$. Resistance ratio with reference to Oregon-R is also shown.

identified, using mass spectrometry to search the NCBI databases for Drosophila matches. Those with a significant ($P < 0.05$) difference in abundance are shown in Table 3. Interestingly, of 9 different proteins identified, 5 are mitochondrially localized. Four proteins, fumarate hydratase, citrate synthase, aconitase, and isocitrate dehydrogenase, are all key enzymes of the tricarboxylic (TCA) cycle and are all upregulated in *Ocd* flies. Taken together this suggests an increase in flux capacity in the TCA cycle, which might support enhanced ATP synthesis. The fact that such a large proportion of the proteins identified in the 2D DIGE study are localized to the mitochondrion is consistent with the original proposal that *Ocd* may play some role in mitochondrial bioenergy metabolism. Alternatively, and in light of the fact that it is known *Ocd* encodes a voltage-gated sodium channel, it may be that the mitochondria alterations provide a route by which symptoms induced by the mutation may be secondarily alleviated.

DISCUSSION

The *Ocd* mutations are alleles of *para*: The mapping, complementation, gene rescue, and gene sequencing data provide compelling evidence that the *Ocd* mutations are alleles of the voltage-gated sodium channel gene *paralytic* (*para*). This is further supported by the observation that the *Ocd* mutations share phenotypes with previously identified *para* alleles, including resistance to DDT and reduced sodium ion current in motor neurons. It is interesting that the possibility of *para* being the host *Ocd* gene was previously excluded (Sondergaard 1975). The critical difference between

TABLE 3

Proteins identified as being differentially expressed in wild-type and *Ocd* flies

MW (kDa)	pI (pH)	Corresponding polypeptide(s)	Function	*P* score from nested ANOVA	Ratio change
			A. Nuclear-encoded mitochondrial genes		
58.0	9.1	CG3861-PB	Citrate synthase	0.0026	+1.57
58.3	9.1	CG3861-PA		0.0266	+1.40
		CG3861-PB			
59.0	9.1	CG3612-PA	ATP synthase α- subunit (Bellwether)	0.00426	+1.39
59.6	9.1	CG3612-PA		0.0147	+1.53
59.6	9.1	CG3612-PA		0.0204	+1.25
59.6	9.1	CG3612-PA		0.0241	+1.45
59.6	9.1	CG3612-PA		0.04951	−1.23
86.2	8.5	CG9244-PB	Aconitase	0.01539	+1.40
54.0	8.6	CG4094-PA	Fumarate hydratase	0.0171	+1.28
		CG4094-PB			
41.0	8.8	CG6439-PA	Isocitrate dehydrogenase β- subunit	0.0381	+1.26
			B. Nonmitochondrial genes		
44.6	5.9	Enolase	Enolase (*Drosophila pseudobscura*)	0.0077	−1.20
41.0	6.3	CG6663-PA	Peptidase inhibitor homolog	0.0104	+1.65
74.3	9.2	CG5939-PC	Paramyosin	0.0241	+1.45
61.7	6.1	CG6148-PA CG6148-PB	Putative achaete scute target 1	0.0270	+1.30

Significant differences in protein abundance are associated with ANOVA *P*-scores of <0.05. Molecular weights (MW) and isoelectric points (pI) are shown. Each entry in the MW column indicates a spot independently identified. Polypeptides are named according to FlyBase nomenclature. In several cases different spots correspond to the same polypeptide which, due to post-translational modification, migrates to a different position on the gel. Proteins were identified by searching the NCBI database. The corresponding polypeptides and encoding genes are listed. The last two columns list the nested ANOVA *P*-values and the ration change. Positive values indicate proteins more abundant in *Ocd* flies; negative values indicate those more abundant in wild type.

previous complementation tests and those reported here is the use of a null *para* allele in a crossing scheme performed at the restrictive cold temperature of 18°.

The *Ocd* mutations are in conserved domains of Para: Sequence analysis revealed two classes of missense mutations that underlie the *Ocd* phenotype, the single missense T1551I mutation unique to Ocd^2, and the double missense I1545M and G1571R mutation which is curiously present in five *Ocd* alleles (Ocd^1, Ocd^3, Ocd^5, Ocd^6, and Ocd^7). These lines were originally reported as being independently derived (Sondergaard 1979), but it is difficult to comprehend how five identical double missense mutations could arise independently, unless the variant was already present in the stock from which the mutants were isolated. Furthermore, while all five I1545M and G1571R stocks have similar dominant cold-sensitivity phenotypes, they do vary in terms of relative male viability and fertility. This strongly suggests that selection for different modifier genes has occurred within the different *Ocd* I1545M and G1571R stocks. All three missense mutations reside within conserved, functionally important parts of the sodium channel protein. Furthermore, analysis of the Para protein and closely related sequences using the SIFT amino acid substitution prediction program (Ng and Henikoff 2001) predicts that each of the *Ocd* mutations (I1545M, T1551I, and G1571R) will affect Para protein function.

The effect of *Ocd* mutations on sodium channel function: The major functional sodium channel in Drosophila is encoded by *para* (Loughney *et al.* 1989). Although both *para* and *DSC1*, a putative voltage-gated sodium channel gene, are widely expressed in the CNS and PNS (Hong and Ganetzky 1994), mutations in *para* are sufficient to block nerve action potentials. For example $para^{Df(1)D34}$, an internal deletion within *para*, abolishes sodium current (Mee *et al.* 2004). Analyses of *SCN4A* derived from myotonic patients show that single-amino-acid substitutions alter the activation threshold and/or rate of fast inactivation (Cannon 2002; Wu *et al.* 2005). *Ocd* larval motor neurons show decreases in peak transient sodium currents, suggesting that the mutant channels are compromised in their ability to transport sodium ions. This might be due to a partial blockage of the sodium channel pore. In *Ocd* flies some sodium current is still present at 16°, indicating that action-potential firing is still occurring at this lower temperature, although it may be slowed or uncoordinated. Further characterization of the electrophysiological phenotype of *Ocd* utilizing heterologous channel expression is likely to establish how such mutations could lead to cold-sensitive sodium channel dysfunction.

Sodium channel function can also be dissected by exposure to neurotoxic insecticides. Indeed, a wide variety of neurotoxins, including DDT and pyrethroids, target Drosophila *para* sodium channels by binding to specific domains within the molecule (Baines and Bate 1998; Zlotkin 1999; Wang and Wang 2003; ffrench-Constant *et al.* 2004). Interestingly, DDT and pyrethroids target *para* sodium channel domain III S6 (Pauron *et al.* 1989), the site of the *Ocd* mutations. Several *para* mutants originally isolated on account of their temperature sensitivity have since been shown to confer insecticide resistance (Pittendrigh *et al.* 1997). This includes $para^{74}$ (M1536I), which also resides in domain III S6 and is known to confer resistance to both DDT and pyrethroids, and $para^{DN7}$ (Pittendrigh *et al.* 1997; ffrench-Constant *et al.* 1998; Martin *et al.* 2000). Pyrethroids and DDT normally function to cause persistent activation of sodium channels (Soderlund and Bloomquist 1989). The fact that viable homozygous Ocd^5 (I1545M and G1571R) females show a 1000-fold increase in resistance to DDT, and heterozygous Ocd^2 (T1551I) females appear to show a mild DDT sensitivity, suggests that the I1545 and/or G1571 residues may be crucial targets for DDT.

***Ocd* and mitochondrial function:** Speculation that the *Ocd* mutation had a mitochondrial function was based on the observation of an unidentified aberrant protein in *Ocd* mitochondria (Sondergaard 1986) and abnormalities in the reaction kinetics of the mitochondrial respiratory chain SCCR activity in *Ocd* mutants (Sondergaard 1976, 1979). Interestingly, changes in the activation energy of mitochondrial enzymes in *para* mutants have also previously been observed (Sondergaard 1976). Using males tightly controlled for genetic background and inbreeding, 40 significant proteomic differences between wild-type and Ocd^7 males were revealed. The 16 identified protein differences represent 10 proteins, 6 of which are mitochondrial. Interestingly 4 of these are critical components of the TCA cycle and the others are the α- and β-subunits of ATP synthase. All are expressed at high levels in Ocd^7 mutant males. If the primary effect of *Ocd* on sodium channel function is to slow inactivation, then there will be an increased influx of sodium ions into the cell. The mitochondria may well respond to this increase in sodium ion concentration by increasing ATP synthesis, specifically by increasing levels of key TCA cycle enzymes and ATP synthase. This would facilitate subsequent energy-dependent clearance of excess intracellular sodium.

***Ocd* as a model of human sodium channel disorders:** Several human disorders associated with myotonia and periodic paralyses are caused by mutations in the skeletal muscle sodium channel *SCN4A* (reviewed by Caldwell and Schaller 1992; Cannon 1997, 2000; George 2005). These include hyperkalemic periodic paralysis (HYPP), paramyotonia congenita (PMC), potassium-aggravated myotonia (PAM), and hypokalemic periodic paralysis (HOKPP). These diseases are inherited in an autosomal dominant fashion and exhibit high penetrance. Symptoms are episodic and vary in severity both within and between affected individuals. *SCN4A* is only expressed at significant levels in skeletal muscle, so there are generally no cardiac or CNS

symptoms in the patients. A plethora of *SCN4A* missense mutations have been described that result in the substitution of a highly conserved amino acid in the protein. In these mutant channels, permeation of sodium ions through the channel pore is apparently normal. The primary defect is instead an alteration in voltage-dependent gating, specifically the disruption of fast inactivation. This manifests itself as aberrant bursts of reopening of the channel and prolonged durations of the open state. Several identified mutations lie in the cytoplasmic loop, linking domains III and IV, which contains the inactivation gate. Other mutations lie at the cytoplasmic ends of S5 or S6, which may form part of the inner part of the ionic pore to which the inactivation gate binds, namely the docking site.

From a human genetic disease perspective the *Ocd* G1571R mutation is of particular interest. The mutated glycine residue is conserved from Drosophila to man and lies very close to the hydrophobic motif MFMT (residues 1576–1579), believed to directly interact with the docking site. Interestingly, mutations in the orthologous residue, G1306, in the human skeletal muscle sodium channel SCN4A, have already been found in cases of the human cold-sensitive muscle disorder paramyotonia congenita (G1306V) (McClatchey *et al.* 1992). It is remarkable that mutations at the same residue result in cold-sensitive phenotypes in both Drosophila and humans. Other *SCN4A* G1306 mutations have been uncovered in two families with potassium-associated myotonia, one of which is associated with a G1306A substitution (Ricker *et al.* 1994), while the second is caused by a G1306E substitution (Lerche *et al.* 1993). To date, no G1306R mutation in *SCN4A* has been reported. The effect of the three *SCN4A* G1306 mutations (G1306A, G1306E, and G1306V) on gating revealed both inactivation and activation defects (Mitrovic *et al.* 1995). The scale of channel defect correlates with the severity of symptoms observed in patients, with G1306A being the least affected and G1306E the most severe. G1306A has also been associated with succinylcholine-induced masseter muscle rigidity, a complication associated with anesthesia that can be fatal.

Cold-sensitive mutations in the human skeletal sodium channel genes, SCN4A, include R1448H and M1360V (Mohammadi *et al.* 2003) and T1313A (Bouhours *et al.* 2004). The molecular mechanisms underlying the temperature sensitivity of this muscle disorder are not well understood. Nevertheless, a decrease in temperature is known to slow down sodium channel kinetics and reduce the number of excitable sodium channels through hyperpolarizing shifts in slow inactivation (Ruff, 1999). Again the precise mechanism by which the R1448H, M1360V, and T1313A mutations induce cold sensitivity of sodium channels has not been elucidated (Yang *et al.* 1994; Mohammadi *et al.* 2003; Bouhours *et al.* 2004).

At present no mammalian model exists for human skeletal muscle (*SCN4A*) disorders. An appropriate genetic model would undoubtedly aid in establishing the mechanisms by which inactivation is disrupted in *SCN4A*-associated sodium channel disorders, and how this disruption may be exacerbated or mitigated by factors such as activity, serum potassium levels, and temperature. Once such interactions are better understood, it should also be possible to develop improved pharmacological treatments.

D. melanogaster models of genetic disease have proven to be invaluable in elucidating the pathogenic mechanisms behind many human disorders (Fortini and Bonini 2000; Kornberg and Krasnow 2000; Zoghbi and Botas 2002; O'Kane 2003; Jacobs *et al.* 2004; Bier 2005; Chintapalli *et al.* 2007). As it is likely that the pathogenic mechanism of sodium channel-mediated cold sensitivity is similar in flies and humans, further characterization of the Drosophila *Ocd* lines should clarify how equivalent human mutations cause disease phenotypes. The *Ocd* lines will also be invaluable in identifying specific chemicals and pharmaceutical products that may be able to alleviate symptoms of human sodium channel dysfunction.

For technical support with mass spectrometry, we thank Julie Howard and Svenja Hester of the Cambridge Centre for Proteomics. Helen A. Lindsay was supported by a Biotechnology and Biological Sciences Research Council Studentship.

LITERATURE CITED

Ashburner, M., 1989 *Drosophila: A Laboratory Manual.* Cold Spring Harbor Laboratory Press, Cold Spring Harbor, NY.

Baines, R. A., and M. Bate, 1998 Electrophysiological development of central neurons in the *Drosophila* embryo. J. Neurosci. **18:** 4673–4683.

Bellen, H. J., R. W. Levis, G. Liao, Y. He, J. W. Carlson *et al.*, 2004 The BDGP gene duplication project: single transposon insertions associated with 40% of Drosophila genes. Genetics **167:** 761–781.

Bier, E., 2005 *Drosophila*, the golden bug, emerges as a tool for human genetics. Nat. Rev. Genet. **6:** 9–23.

Bonini, N. N., Q. T. Bui, G. L. Gray-Board and J. M. Warrick, 1997 The *Drosophila eyes absent* gene directs ectopic eye formation in a pathway conserved between flies and vertebrates. Development **124:** 4819–4826.

Bouhours, M., S. Luce, D. Sternberg, J. C. Willer, B. Fontaine *et al.*, 2004 A1152D mutation of the Na^+ channel causes paramyotonia congenita and emphasizes the role of DIII/S4–S5 linker in fast inactivation. J. Physiol. **565:** 415–427.

Broadie, K., and M. Bate, 1993 Activity-dependent development of the neuromuscular synapse during *Drosophila* embryogenesis. Neuron **11:** 607–619.

Caldwell, J. H., and K. L. Schaller, 1992 Opening the gates on ion channel diseases. Nat. Genet. **2:** 87–89.

Cannon, S. C., 1997 From mutation to myotonia in sodium channel disorders. Neuromuscul. Disord. **7:** 241–249.

Cannon, S. C., 2000 Spectrum of sodium channel disturbances in the nondystrophic myotonias and periodic paralyses. Kidney Int. **57:** 772–779.

Cannon, S. C., 2002 An expanding view for the molecular basis of familial periodic paralysis. Neuromuscul. Disord. **12:** 533–543.

Chintapalli, V. R., J. Wang and J. A. T. Dow, 2007 Using FlyAtlas to identify better *Drosophila* melanogaster models of human disease. Nat. Genet. **39:** 715–720.

Dellinger, B., R. Felling and R. W. Ordway, 2000 Genetic modifiers of the Drosophila NSF mutant, *comatose*, include a temper-

ature-sensitive paralytic allele of the calcium hannel α1-subunit gene, *cacophony*. Genetics **155:** 203–211.

Feng, Y., L. Huynh, K. Takeyasu and D. M. Fambrough, 1997 The *Drosophila* Na,K-ATPase alpha-subunit gene: gene structure, promoter function and analysis of a cold-sensitive recessive-lethal mutation. Genes Funct. **1:** 99–117.

ffrench-Constant, R. H., B. Pittendrigh, A. Vaughan and N. Anthony, 1998 Why are there so few resistance-associated mutations in insecticide target genes. Philos. Trans. R. Soc. Lond. B. **353:** 1685–1693.

ffrench-Constant, R. H., P. J. Daborn and G. Le Goff, 2004 The genetics and genomics of insecticide resistance. Trends Genet. **20:** 163–170.

Fortini, M. E., and N. M. Bonini, 2000 Modeling human neurodegenerative diseases in *Drosophila*. Trends Genet. **16:** 161–167.

George, A. L., 2005 Inherited disorders of voltage-gated sodium channels. J. Clin. Invest. **115:** 1990–1999.

Homyk, T., and Q. Pye, 1989 Some mutations affecting neural or muscular tissues alter the physiological components of the electroretinogram in *Drosophila*. J. Neurogenet. **5:** 37–48.

Hong, C-S., and B. Ganetzky, 1994 Spatial and temporal expression patterns of two sodium channel genes in *Drosophila*. J. Neurosci. **14:** 5160–5169.

Jacobs, H. T., D. J. M. Fernandez-Ayala, S. Manjiry, E. Kemppainen, J. M. Toivonen *et al.*, 2004 Mitochondrial disease in flies. Biochim. Biophys. Acta **1659:** 190–196.

Jarman, A. P., Y. Grau, L. Y. Yan and Y. N. Jan, 1993 *atonal* is a proneural gene that directs chordotonal organ formation in the *Drosophila* peripheral nervous system. Cell **73:** 1307–1321.

Karp, N. A., M. Spencer, H. Lindsay, K. M. C. O'Dell and K. S. Lilley, 2005 Impact of replicate types on proteomic expression analysis. J. Prot. Res. **4:** 1867–1871.

Kawasaki, F., R. Felling and R. W. Ordway, 2000 A temperature-sensitive paralytic mutant defines a primary synaptic calcium channel in *Drosophila*. J. Neurosci. **20:** 4885–4889.

Kornberg, T. B., and M. A. Krasnow, 2000 The *Drosophila* genome sequence: implications for biology and medicine. Science **287:** 2218–2220.

Lerche, H., R. Heine, U. Pika, A. L. George, N. Mitrovic *et al.*, 1993 Human sodium channel myotonia: slowed channel inactivation due to substitutions for a glycine within the III–IV linker. J. Physiol. **470:** 13–22.

Lilly, M., J. Riesgo-Escovar and J. Carlson, 1994 Developmental analysis of the *smellblind* mutants: evidence for the role of sodium channels in *Drosophila* development. Dev. Biol. **162:** 1–8.

Loughney, K., R. Kreber and B. Ganetzky, 1989 Molecular analysis of the *para* locus, a sodium channel gene in *Drosophila*. Cell **58:** 1143–1154.

Martin, R. L., B. Pittendrigh, J. Liu, R. Reenan, R. ffrench-Constant and D. A. Hanck, 2000 Point mutations in domain III of a Drosophila neuronal Na channel confer resistance to allethrin. Insect Biochem. Mol. Biol. **30:** 1051–1059.

McClatchey, A. I., P. Van den Bergh, M. A. Pericak-Vance, W. Raskind, C. Verellen *et al.*, 1992 Temperature-sensitive mutations in the III–IV cytoplasmic loop region of the skeletal muscle sodium channel gene in Paramyotonia congenita. Cell **68:** 769–774.

Mee, C. J., E. C. G. Pym, K. G. Moffat and R. A. Baines, 2004 Regulation of neuronal excitability through *pumilio*-dependent control of a sodium channel gene. J. Neurosci. **24:** 8695–8703.

Mitrovic, N., A. L. George, H. Lerche, S. Wagner, C. Fahlke *et al.*, 1995 Different effects on gating of three myotonia-causing mutations in the inactivation gate of the human muscle sodium channel. J. Physiol. **487:** 107–114.

Mohammadi, B., N. Mitrovic, F. Lehmann-Horn, R. Dengler and J. Bufler, 2003 Mechanisms of cold sensitivity of paramyotonia congenita mutation R1448H and overlap syndrome mutation M1360V. J. Physiol. **547:** 691–698.

Ng, P. C., and S. Henikoff, 2001 Predicting deleterious amino acid substitutions. Genome Res. **11:** 863–874.

O'Kane, C. J., 2003 Modelling human diseases in *Drosophila* and *Caenorhabditis*. Sem. Cell Dev. Biol. **14:** 3–10.

Ordway, R. W., L. Pallanck and B. Ganetzky, 1994 Neurally expressed *Drosophila* genes encoding homologs of the NSF and SNAP proteins. Proc. Natl. Acad. Sci. USA **91:** 5715–5719.

Pauron, D., J. Barhanin, M. Amichot, M. Pralavorio, J-B. Berge *et al.*, 1989 Pyrethroid receptor in the insect Na^+ channel: alteration of its properties in pyrethroid-resistant flies. Biochemistry **28:** 1673–1677.

Pittendrigh, B., R. Reenan, R. H. ffrench-Constant and B. Ganetzky, 1997 Point mutations in the *Drosophila* sodium channel gene *para* associated with resistance to DDT and pyrethroid insecticides. Mol. Gen. Genet. **256:** 602–610.

Ptacek, L. J., A. L. George, R. L. Barchi, R. C. Griggs, J. E. Riggs *et al.*, 1992 Mutations in an S4 segment of the adult skeletal muscle sodium channel cause Paramyotonia congenita. Neuron **8:** 891–897.

Ranganayakulu, G., R. A. Schulz and E. N. Olson, 1996 Wingless signaling induces *nautilius* expression in the ventral mesoderm of the *Drosophila* embryo. Dev. Biol. **176:** 143–148.

Ricker, K., R. T. Moxley, R. Heine and F. Lehmann-Horn, 1994 Myotonia fluctuans. A third type of muscle sodium channel disease. Arch. Neurol. **51:** 1095–1102.

Robertson, J. L., R. M. Russell and N. E. Savin, 1980 POLO: a user's guide to probit or logic analysis. US Forestry Service Technical Report. Pacific Southwest Research Station, Albany, CA.

Ruff, R., 1999 Effects of temperature on slow and fast inactivation of rat skeletal muscle Na^+ channels. Am. J. Physiol. **277:** C937–C947.

Scholz, H., M. Franz and U. Heberlein, 2005 The *hangover* gene defines a stress pathway required for ethanol tolerance development. Nature **436:** 845–847.

Siddiqi, O., and S. Benzer, 1976 Neurophysiological defects in temperature-sensitive paralytic mutants of *Drosophila melanogaster*. Proc. Natl. Acad. Sci. USA **73:** 3253–3257.

Soderlund, D. M., and J. R. Bloomquist, 1989 Neurotoxic actions of pyrethroid insecticides. Annu. Rev. Entomol. **34:** 77–96.

Sondergaard, L., 1975 A temperature-sensitive behavioural mutant of *Drosophila melanogaster*: *Out-cold*. Hereditas **81:** 199–210.

Sondergaard, L., 1976 Temperature-induced changes in succinate-cytochrome *c* reductase in behavioral mutants of *Drosophila*. Hereditas **82:** 51–56.

Sondergaard, L., 1979 Dominant cold paralytic mutations on the X-chromosome *of Drosophila melanogaster*. Hereditas **90:** 93–101.

Sondergaard, L., 1980 Dominant cold paralytic mutations on the autosomes of *Drosophila melanogaster*. Hereditas **92:** 335–340.

Sondergaard, L., 1986 The nuclear mutation $Ocd^{ts\text{-}1}$ changes the 2-D electrophoretic pattern of *Drosophila* mitochondria. Hereditas **104:** 313–315.

Sondergaard, L., N. C. Nielsen and R. M. Smillie, 1975 The effect of the $Out\text{-}cold^{ts}$ mutation on temperature induced changes in the Arrhenius activation energy of succinate-cytochrome *c* reductase activity in *Drosophila*. FEBS Lett. **51:** 126–129.

Suzuki, D. T., T. Grigliatti and R. Williamson, 1971 Temperature-sensitive mutations in *Drosophila melanogaster*, VII. A mutation ($para^{ts}$) causing reversible adult paralysis. Proc. Natl. Acad. Sci. USA **68:** 890–893.

Swatton, J. E., S. Prabakaran, N. A. Karp, K. S. Lilley and S. Brahn, 2004 Protein profiling of human postmortem brain using 2-dimensional fluorescence difference gel electrophoresis (2-D DIGE). Mol. Psych. **9:** 128–143.

Sweeney, S. T., K. Broadie, J. Keane, H. Niemann and C. O'Kane, 1995 Targeted expression of tetanus toxin light chain in *Drosophila* specifically eliminates synaptic transmission and causes behavioral defects. Neuron **14:** 341–351.

Wang, S-Y., and G. K. Wang, 2003 Voltage-gated sodium channels as primary targets of diverse lipid-soluble neurotoxins. Cell. Signal. **15:** 151–159.

Warmke, J. W., R. A. G. Reenan, P. Wang, S. Qian, J. P. Arena *et al.*, 1997 Functional expression of *Drosophila para* sodium channels modulation by the membrane protein TipE and toxin pharmacology. J. Gen. Physiol. **110:** 119–133.

Wodarz, A., U. Hinz, M. Engelbert and E. Knust, 1995 Expression of *crumbs* confers apical character on plasma membrane domains of ectodermal epithelia of *Drosophila*. Cell **82:** 67–76.

Wu, F-F., E. Gordon, E. P. Hoffman and S. C. Cannon, 2005 A C-terminal skeletal muscle sodium channel mutation associated with myotonia disrupts fast inactivation. J. Physiol. **565:** 371–380.

Yang, N., S. Si, M. Zhou, L. J. Ptacek, R. L. Barchi *et al.*, 1994 Sodium channel mutations in paramyotonia congenita exhibit similar biophysical phenotypes in vitro. Proc. Natl. Acad. Sci. USA **91:** 12785–12789.

Zhai, G. G., P. R. Hiesinger, T-W. Koh, P. Verstreken, K. L. Schulze *et al.*, 2003 Mapping *Drosophila* mutations with molecularly defined *P* element insertions. Proc. Natl. Acad. Sci. USA **100:** 10860–10865.

Zlotkin, E., 1999 The insect voltage-gated sodium channel as target of insecticides. Annu. Rev. Entomol. **44:** 429–455.

Zoghbi, H. Y., and J. Botas, 2002 Mouse and fly models of neurodegeneration. Trends Genet. **18:** 463–471.

Communicating editor: R. Anholt